Archives of Civil and Mechanical Engineering (2021) 21:64
https://doi.org/10.1007/s43452-021-00214-6

ORIGINAL ARTICLE

Modified Burzynski criterion along with AFR and non-AFR for asymmetric anisotropic materials

Farzad Moayyedian[1] · **Mehran Kadkhodayan**[2]

Received: 24 December 2020 / Revised: 18 February 2021 / Accepted: 16 March 2021

Abstract

Burzynski criterion is a well-known criterion is employed for pressure-sensitive isotropic materials. In the current study, this criterion is modified for asymmetric anisotropic materials called hear MB. Firstly, a modified deviatoric stress tensor is defined with a linear transformation to consider the anisotropy effects of materials. Secondly, MB is presented by the sum of *n*-components to have more capability to be calibrated with different numbers of experimental tests and thirdly, the non-linear impact of hydrostatic pressure is ignored due to the previous experiments. In this research, when associated flow rule (AFR) and non-associated flow rule (non-AFR) are employed to calibrate MB, it is called MB-1 and MB-2, respectively. Yielding of different alloys such as AA 2008-T4 and AA 2090-T3 with Face-Centered Cubic (FCC) structure and also AZ31 B, ZK61 M, high purity α-titanium, texture magnesium, Mg-0.5% Th alloy, Mg-4% Li alloy and Ti-4 Al-1/4 O_2 titanium alloy with Hexagonal Close-Packed (HCP) structure are studied to show the accuracy of MB-1 and MB-2. It is shown that the presented approach is very effective especially by using MB-2.

Keywords Burzynski criterion · Asymmetric anisotropic materials · Hydrostatic pressure · Sum of n-components · FCC · HCP · AFR and non-AFR

1 Introduction

Accurate modeling of anisotropic plastic deformation has been one of the key issues in sheet metal forming researches. Dozens of yield functions were developed with different accuracy and distinct applications for depicting the mechanical behavior of asymmetric anisotropic materials. Here, the issue of pressure sensitivity/insensitivity, strength differential in tension and compression, and different criteria such as the Burzynski criterion are reviewed, briefly.

Spitzig et al. [1] examined the stress–strain behavior of quenched and tempered AISI 4310 and 4330 steel in tension and compression. The results showed that the yield and flow stresses were sensitive to hydrostatic pressure. Spitzig and Richmond [2] presented experimental results on iron-based materials and on aluminum and showed that the flow stress was a linear function of pressure. Barlat et al. [3] proposed a plane stress yield function to predict the anisotropic behavior of sheet metals, in particular, aluminum alloy sheets. The anisotropy of the function was introduced in the formulation using two linear transformations on the Cauchy stress tensor. Stoughton and Yoon [4] suggested a non-AFR based on a pressure-sensitive yield criterion with isotropic hardening that was consistent with the Spitzig and Richmond data and analysis [2]. Hu [5] suggested an anisotropic yield criterion that was derived with the use of invariants of the stress tensor.

Pecherski [6] studied the Burzynski criterion about considering asymmetry in the elastic range and the position of Burzynski's energy-based approach. Hu and Wang [7] proposed a constitutive model characterized experimentally via two steps, one related to the yielding behavior, and the other to the plastic flow of deformation. Stoughton and Yoon [8] described a non-AFR model based on explicit integration of the yield criterion in the closed-form. Nixon et al. [9] presented an experimental and theoretical investigation into the deformation of high-purity and polycrystalline a-titanium.

✉ Farzad Moayyedian
farzad.moayyedian@eqbal.ac.ir

Mehran Kadkhodayan
kadkhoda@um.ac.ir

1 Department of Mechanical Engineering, Eqbal Lahoori Institute of Higher Education, Mashhad, Iran

2 Department of Mechanical Engineering, Ferdowsi University of Mashhad, Mashhad, Iran

Fras et al. [10] and Fras and Pecherski [11] discussed several criteria based on the energy-based hypothesis Burzynski criterion. Vadillo et al. [12] formulated an implicit integration of the elastic–plastic constitutive equations for the paraboloid case of Burzynski's yield condition.

Nowak et al. [13] discussed a proposition of an energy-based hypothesis effort for isotropic materials exhibiting strength-differential effect, pressure-sensitivity, and Lode angle dependence. Pecherski et al. [14] proposed an extension of the Burzynski hypothesis to account the influence of the third invariant of stress tensor deviator. The contribution of the density of elastic energy of distortion in the material effort was controlled by Lode angle. Szeptynski [15] discussed misstatements appearing in the final form of the failure criterion formulation, derived from Burzynski's hypothesis for anisotropic bodies. Furthermore, propositions of different formulation of the failure criterion, basing on the original ideas of Burzynski, were given. Ostrowska- Maciejewska et al. [16] based on the concept of influence functions introduced by Burzynski and on the concept of decomposition of elastic energy density introduced a proposition of an energy-based hypothesis of material effort. The proposition enabled the description of a wide class of linearly elastic materials of arbitrary symmetry exhibiting strength differential effect (SDE).

Andar et al. [17] tested a commercial AZ31 magnesium alloy sheet under uniaxial tension/compression loading and proportional biaxial tensile loading using cruciform specimens. Lou et al. [18] extended the symmetric yield functions for the consideration of SDE in sheet metals. The SDE was coupled with symmetric yield functions by adding a weighted pressure term for the anisotropic materials based on the approaches of Spitzig et al. [1], Spitzig and Richmond [2] and Stoughton and Yoon [4]. Yoon et al. [19] proposed a general asymmetric yield function with dependence on the stress invariants for pressure-sensitive metals. The pressure sensitivity of the proposed yield function was consistent with the experimental result of Spitzig and Richmond [2] for the steel and aluminum alloys while the asymmetry of the third invariant was preserved to model SDE of pressure insensitive materials.

Moayyedian and Kadkhodayan [20] presented a non-AFR criterion to model the behavior of the anisotropic asymmetric sheet metals. In their model, the modified Yld2000-2d proposed by Lou et al. [16] was considered as yield function and the Yld2000-2d proposed by Barlat et al. [3] was considered as plastic potential function. Moayyedian and Kadkhodayan [21, 24] also developed the Burzynski criterion for the anisotropic asymmetric metals with non-AFR and AFR for plane stress problems. Kolupaev et al. [22] formulated some limit surfaces based on the concept of equivalent stress. These hypotheses took into account not only existing information from the experimental tests but they could also describe experiences and different expectations concerning the material behavior mathematically. Later on, Moayyedian and Kadkhodayan [23] presented an advanced criterion with non-AFR for depicting the behavior of anisotropic sheet metals to consider the SDEs. Yield and plastic potential functions of advanced criterion depended on the structure of an anisotropic material (i.e. BCC, FCC and HCP). Lou and Yoon [25] proposed an anisotropic ductile fracture criterion for the ductile fracture of lightweight metals. The ductile fracture criterion coupled effect of stress triaxiality on void growth and assumed the shear linking-up of voids governed by the largest shear stress.

Moreover, Moayyedian and Kadkhodayan [26] investigated into the non-linear influence of hydrostatic pressure on the yielding of asymmetric anisotropic sheet metals. Suzuki et al. [27] investigated the circular and oval hole expansion behaviors of JSH440W and JSH590R high-strength steel sheets based on experiments and FE simulations using three types of anisotropic yield functions: Hill48-r, Yld2000-2d, and 6-poly models. Lou and Yoon [28] analyzed the effect of the third stress invariant in the Drucker function and calibrated it for the metals with body-centered cubic (BCC) and face-centered cubic (FCC) crystal systems. Mucha et al. [29] determined the influence of some factors on the localization phenomena which could result from geometrical, material and thermal softening. Chandola et al. [30] predicted the effect of texture on the plastic anisotropy and consequently the drawing performance of polycrystalline metallic sheets. Lou et al. [31] revisited Yld2004-18p function and modified it to provide satisfactory predictability of orthotropic behavior of BCC and FCC materials under spatial loading. Lia et al. [32] investigated the mechanical properties, especially the yield behavior of AZ31B and ZK61M magnesium alloys. Lou and Yoon [33] developed an anisotropic ductile fracture criterion by introducing anisotropic parameters into the weight function of an uncoupled shear ductile fracture criterion. Wosatko [34] reviewed the role of the dilatancy angle in pressure-dependent plasticity models. It was showed that the definitions of the angle in the CDP model and in the Burzynski-Drucker-Prager plasticity model for a continuum could lead to different angle magnitudes. Banaszkiewicz et al. [35] presented the results of experimental tests and numerical simulations about SDE. The SD parameter was then used in the formula for equivalent stress proposed by Burzynski. The material effort calculated using Burzynski and Huber-Mises-Hencky hypotheses was compared for different start-stop cycles. It was finally shown that the SDE has a significant influence on the predicted fatigue life under thermo-mechanical loading. Wu et al. [36] developed an anisotropic constitutive model based on non-AFR and combined it with non-quadratic and quadratic functions for orthotropic anisotropic sheet metals.

In the current study, the Burzynski criterion used for isotropic materials is modified for the asymmetric anisotropic materials and called hear MB. Modified deviatoric stress tensor with a linear transformation is defined to consider the anisotropy behavior of materials. The MB is presented in the form of sum of n-components to have more capability to be calibrated with different numbers of experimental tests. The non-linear impact of hydrostatic pressure is neglected due to the previous experiments. Moreover, yielding of different alloys such as AA 2008-T4 and AA 2090-T3 with Face-Centered Cubic (FCC) structure and also AZ31 B, ZK61 M, high purity α-titanium, texture magnesium, Mg-0.5% Th alloy, Mg-4% Li alloy and Ti-4 Al-1/4 O2 titanium alloy with Hexagonal Close-Packed (HCP) structure are studied to show the accuracy of the MB.

2 Burzynski criterion

In this part, the Burzynski criterion is extended from isotropic to anisotropic materials with AFR and non-AFR. It is notified that the non-linear effect of hydrostatic pressure is omitted in MB.

2.1 MB-1 for anisotropic materials with AFR

To define MB for the anisotropic materials a transformation matrix is needed with the coefficients of $c_i'(i = 1 - 6)$ obtained by experimental results in different rolling directions. The matrix is implied to stress tensor σ_{ij} to obtain modified deviatoric stress tensor for anisotropic materials, $\hat{s}_{ij}$ as in Eq. (1) [28].

Now, the first invariant of modified stress tensor and the second invariant of modified deviatoric stress tensor for anisotropic materials can be presented accordingly in Eq. (2). Finally, the yield function of MB-1 with the inspiration of [28] is proposed in Eq. (3). For the plane stress problems $\left(\sigma_{zz} = \tau_{yz} = \tau_{xz} = 0\right)$ the modified hydrostatic pressure and the second invariant of modified deviatoric stress tensor are as Eq. (4). where, a_1', a_2', a_3' and a_6' are in Eq. (5).

$$\begin{Bmatrix} \hat{s}_{xx} \\ \hat{s}_{yy} \\ \hat{s}_{zz} \\ \hat{s}_{yz} \\ \hat{s}_{xz} \\ \hat{s}_{xy} \end{Bmatrix} = \begin{bmatrix} \frac{(c_2'+c_3')}{3} & -\frac{c_3'}{3} & -\frac{c_2'}{3} & 0 & 0 & 0 \\ -\frac{c_3'}{3} & \frac{(c_1'+c_3')}{3} & -\frac{c_1'}{3} & 0 & 0 & 0 \\ -\frac{c_2'}{3} & -\frac{c_1'}{3} & \frac{(c_1'+c_2')}{3} & 0 & 0 & 0 \\ 0 & 0 & 0 & c_4' & 0 & 0 \\ 0 & 0 & 0 & 0 & c_5' & 0 \\ 0 & 0 & 0 & 0 & 0 & c_6' \end{bmatrix} \begin{Bmatrix} \sigma_{xx} \\ \sigma_{yy} \\ \sigma_{zz} \\ \tau_{yz} \\ \tau_{xz} \\ \tau_{xy} \end{Bmatrix} \quad (1)$$

$$\begin{cases} \hat{I}_1 = d_{xx}\sigma_{xx} + d_{yy}\sigma_{yy} + d_{zz}\sigma_{zz} \\ \hat{J}_2 = \frac{1}{2}\hat{s}_{ij}\hat{s}_{ij} = -\hat{s}_{xx}\hat{s}_{yy} - \hat{s}_{yy}\hat{s}_{zz} - \hat{s}_{xx}\hat{s}_{zz} + \hat{s}_{xy}^2 + \hat{s}_{yz}^2 + \hat{s}_{xz}^2 \end{cases} \quad (2)$$

$$\sigma_y\left(\sigma_{ij}\right) = \frac{1}{n}\sum_{i=1}^{n}\left\{\hat{A}\left[\hat{J}_2^{(i)}\right] + \hat{B}\left[\hat{I}_1^{(i)}\right]^2 + \left[\hat{I}_1^{(i)}\right] - 1\right\} = 0 \quad (3)$$

$$\begin{cases} \hat{I}_1 = d_{xx}\sigma_{xx} + d_{yy}\sigma_{yy} \\ \hat{J}_2 = \frac{1}{2}\hat{s}_{ij}\hat{s}_{ij} = a_1'\sigma_{xx}^2 + a_2'\sigma_{xx}\sigma_{yy} + a_3'\sigma_{yy}^2 + a_6'\tau_{xy}^2 \end{cases} \quad (4)$$

With considering $\hat{A} = 1$ for simplicity and $\hat{B} = 0$ to neglect the non-linear impact of hydrostatic pressure, in Eq. (3), the yield function of MB-1 is stated as in Eq. (6). This criterion has the following three benefits:

1. It is extended from an isotropic criterion to an anisotropic one.
2. It is presented by the sum of n-components to have more capability to be calibrated with different numbers of experimental tests.
3. The non-linear impact of hydrostatic pressure is omitted according to [1, 2] implied that the yielding of anisotropic aluminum and magnesium alloys are dependent linearly on hydrostatic pressure.

$$\begin{cases} a_1' = \dfrac{c_2'^2 + c_3'^2 + c_2'c_3'}{9} \\ a_2' = \dfrac{c_1'c_2' - c_1'c_3' - c_2'c_3' - 2c_3'^2}{9} \\ a_3' = \dfrac{c_1'^2 + c_3'^2 + c_1'c_3'}{9} \\ a_6' = c_6'^2 \end{cases} \quad (5)$$

$$\sigma_y\left(\sigma_{ij}\right) = \frac{1}{n}\sum_{i=1}^{n}\left[\hat{J}_2^{(i)} + \hat{I}_1^{(i)} - 1\right] = 0 \quad (6)$$

Finally, the yield function of MB-1 in Eq. (6) with the aid of Eqs. (4) and (5) for plane stress problems can be rewritten as:

$$\sigma_y\left(\sigma_{ij}\right)=\frac{1}{n}\left\{\begin{array}{l}\left[\begin{array}{l}\sum_{i=1}^{n}\left(a_1'\right)^{(i)}\sigma_{xx}^2+\sum_{i=1}^{n}\left(a_2'\right)^{(i)}\sigma_{xx}\sigma_{yy}+\\ \sum_{i=1}^{n}\left(a_3'\right)^{(i)}\sigma_{yy}^2+\sum_{i=1}^{n}\left(a_6'\right)^{(i)}\tau_{xy}^2\end{array}\right]+\\ \left[\sum_{i=1}^{n}\left(d_{xx}\right)^{(i)}\sigma_{xx}+\sum_{i=1}^{n}\left(d_{yy}\right)^{(i)}\sigma_{yy}\right]-n\end{array}\right\}=0 \tag{7}$$

Moreover, the derivatives of yield function with respect to stress components (i.e. $\frac{\partial\sigma_y}{\partial\sigma_{xx}}, \frac{\partial\sigma_y}{\partial\sigma_{yy}}, \frac{\partial\sigma_y}{\partial\sigma_{xy}}$ are computed here employed in the calibration of MB-1:

$$\begin{cases}\frac{\partial\sigma_y}{\partial\sigma_{xx}}=\frac{1}{n}\left\{\left[2\sum_{i=1}^{n}\left(a_1'\right)^{(i)}\sigma_{xx}+\sum_{i=1}^{n}\left(a_2'\right)^{(i)}\sigma_{yy}\right]+\left(\sum_{i=1}^{n}\left(d_{xx}\right)^{(i)}\right)\right\}\\ \frac{\partial\sigma_y}{\partial\sigma_{yy}}=\frac{1}{n}\left\{\left[\sum_{i=1}^{n}\left(a_2'\right)^{(i)}\sigma_{xx}+2\sum_{i=1}^{n}\left(a_3'\right)^{(i)}\sigma_{yy}\right]+\left(\sum_{i=1}^{n}\left(d_{yy}\right)^{(i)}\right)\right\}\\ \frac{\partial\sigma_y}{\partial\tau_{xy}}=\frac{1}{n}\left(2\sum_{i=1}^{n}\left(a_6'\right)^{(i)}\tau_{xy}\right)\end{cases} \tag{8}$$

It is noted that due to using AFR, the yield and plastic potential functions are similar here (i.e. $\sigma_p=\sigma_y$).

2.2 MB-2 for anisotropic materials with non-AFR

While using non-AFR, the plastic potential function is different from the yield function. The proposed plastic potential function linearly depends on hydrostatic pressure. A transformation matrix is used and the $c_i''(i=1-6)$ are coefficients obtained by experimental results in different rolling directions. The matrix is implied to stress tensor σ_{ij} to attain modified deviatoric stress tensor for anisotropic materials, therefore, s_{ij}'' and c_i'' can be inserted instead of $\hat{s}_{ij}$ and c_i' in Eq. (1). The first invariant of modified stress tensor and the second invariant of modified deviatoric stress tensor for anisotropic materials, so $\overline{I}_1$, $\overline{J}_2$, $\overline{d}_i$ and s_{ij}'' can be replaced by $\hat{I}_1$, $\hat{J}_2$, d_i and $\hat{s}_{ij}$, respectively, in Eq. (2). Now, the plastic potential function of MB-2 can be introduced with substituting σ_p, $\overline{I}_1$, $\overline{J}_2$,$\overline{A}$, $\overline{B}$ instead of σ_y, $\hat{I}_1$, $\hat{J}_2$ $\hat{A}$, $\hat{B}$ in Eq. (3). For the plane stress problems, $\hat{I}_1$, $\hat{J}_2$, s_{ij}'', $\overline{a}_i$, $\overline{d}_i$ are placed instead of $\hat{I}_1$, $\hat{J}_2$, $\hat{s}_{ij}$, a_i', d_i in Eq. (4) in which, $\overline{a}_i$ are computed as in Eq. (5) with inserting c_i'' with c_i'. With considering $\overline{A}=1$ for simplicity and $\overline{B}=0$ to neglect the non-linear impact of hydrostatic pressure, the plastic function of MB-2 can be stated with replacing σ_y, $\hat{I}_1$, $\hat{J}_2$, by σ_p, $\overline{I}_1$, $\overline{J}_2$ in Eq. (6). Hence, the plastic function of MB-2 can be simplified with inserting σ_p, $\overline{a}_i$, $\overline{d}_i$ instead of σ_y, $\hat{a}_i$, d_i in Eq. (7) for the plane stress problems. In addition, the derivatives can be used for calibration of plastic potential function with substituting σ_p, $\overline{a}_i$, $\overline{d}_i$ instead of σ_y, $\hat{a}_i$, d_i in Eq. (8). It is clear that due to using non-AFR, the yield and plastic potential functions are different here (i.e. $\sigma_p \neq \sigma_y$).

3 Calibration of MB-1 and MB-2

In order to calibrate the MB-1, with $n=i$, $i=1,2,3,\ldots$, $6\times i$ experimental results are required to obtain constants of $\left(c_1'\right)^i$, $\left(c_2'\right)^i$, $\left(c_3'\right)^i$, $\left(c_6'\right)^i$, $\left(d_x\right)^i$, $\left(d_y\right)^i$ in the yield function, and also in MB-2 with $n=i$, $i=1,2,3,\ldots,6\times i$ experimental results are necessary to attain constants of $\left(c_1'\right)^i$, $\left(c_2'\right)^i$, $\left(c_3'\right)^i$, $\left(c_6'\right)^i$, $\left(d_x\right)^i$, $\left(d_y\right)^i$ in the yield function. Finally, $6\times i$ experimental results for finding the constants of $\left(\overline{c}_1\right)^i$, $\left(\overline{c}_2\right)^i$, $\left(\overline{c}_3\right)^i$, $\left(\overline{c}_6\right)^i$, $\left(\overline{d}_x\right)^i$, $\left(\overline{d}_y\right)^i$ in the plastic potential function are needed.

In many anisotropic materials, the mechanical properties in different directions from the rolling direction (θ) are differs in tension and compression and, therefore, the following statements are mentioned. For tensile yield stresses tests in the direction θ, it is found that:

$$\begin{cases}\sigma_{xx}=\sigma_\theta^T\cos^2\theta\\ \sigma_{yy}=\sigma_\theta^T\sin^2\theta\\ \tau_{xy}=\sigma_\theta^T sin\theta\cos\theta\end{cases} \tag{9}$$

with substituting Eq. (9) into Eq. (7) we have:

$$A_\theta\left(\sigma_\theta^T\right)^2+B_\theta\left(\sigma_\theta^T\right)-1=0 \tag{10}$$

in which,

$$\begin{cases}A_\theta=\frac{1}{n}\sum_{i=1}^{n}\left\{\left(a_1'\right)^{(i)}\cos^4\theta+\left[\left(a_2'\right)^{(i)}+\left(a_6'\right)^{(i)}\right]\sin^2\theta\cos^2\theta+\left(a_3'\right)^{(i)}\sin^4\theta\right\}\\ B_\theta=\frac{1}{n}\sum_{i=1}^{n}\left[\left(d_{xx}\right)^{(i)}\cos^2\theta+\left(d_{yy}\right)^{(i)}\sin^2\theta\right]\end{cases} \tag{11}$$

Finally, it is obtained that:

$$\sigma_\theta^T = \frac{-B_\theta + \sqrt{B_\theta^2 + 4A_\theta}}{2A_\theta} \tag{12}$$

For compressive yield stresses tests it is found that:

$$\begin{cases} \sigma_{xx} = -\sigma_\theta^C \cos^2\theta \\ \sigma_{yy} = -\sigma_\theta^C \sin^2\theta \\ \tau_{xy} = -\sigma_\theta^C sin\theta \cos\theta \end{cases} \tag{13}$$

and with substituting Eq. (13) into Eq. (7) it is obtained:

$$A_\theta\left(\sigma_\theta^C\right)^2 - B_\theta\sigma_\theta^C - 1 = 0 \tag{14}$$

after simplification, it is found:

$$\sigma_\theta^C = \frac{B_\theta + \sqrt{B_\theta^2 + 4A_\theta}}{2A_\theta} \tag{15}$$

For equi-biaxial tensile yield stress, the stress components are as Eq. (16). With substituting Eq. (16) into Eq. (7), Eq. (17) is found in which A_b and B_b are as Eq. (18). Now, σ_b^T is calculated by Eq. (19).

$$\begin{cases} \sigma_{xx} = \sigma_b^T \\ \sigma_{yy} = \sigma_b^T \\ \tau_{xy} = 0 \end{cases} \tag{16}$$

$$A_b\left(\sigma_b^T\right)^2 + B_b\sigma_b^T - 1 = 0 \tag{17}$$

$$\begin{cases} A_b = \frac{1}{n}\sum_{i=1}^{n}\left\{\left(a_1'\right)^{(i)} + \left(a_2'\right)^{(i)} + \left(a_3'\right)^{(i)}\right\} \\ B_b = \frac{1}{n}\sum_{i=1}^{n}\left[\left(d_{xx}\right)^{(i)} + \left(d_{yy}\right)^{(i)}\right] \end{cases} \tag{18}$$

$$\sigma_b^T = \frac{-B_b + \sqrt{B_b^2 + 4A_b}}{2A_b} \tag{19}$$

For the equi-biaxial compressive yield stress test we have:

$$\begin{cases} \sigma_{xx} = -\sigma_b^C \\ \sigma_{yy} = -\sigma_b^C \\ \tau_{xy} = 0 \end{cases} \tag{20}$$

with inserting Eq. (20) into Eq. (7), it is found that:

$$A_b\left(\sigma_b^C\right)^2 - B_b\sigma_b^C - 1 = 0 \tag{21}$$

and finally it is obtained as:

$$\sigma_b^C = \frac{B_b + \sqrt{B_b^2 + 4A_b}}{2A_b} \tag{22}$$

3.1 Calibration of MB-1

Increments of plastic strains is computed with aid of yield function of Eq. (7), [24]. Uniaxial and equi-biaxial Lankford ratios are defined as Eqs. (23) and (24) based on the biaxial tensile or compressive yield stress. R_θ^T and R_b^T are achieved by inserting Eqs. (12) and (19) into Eqs. (23) and (24) and R_θ^C and R_b^C are attained from substituting Eqs. (15) and (22) into Eqs. (23) and (24).

$$R_\theta = \frac{d\varepsilon_{yy}^p}{d\varepsilon_{zz}^p} = -\frac{d\varepsilon_{yy}^p}{d\varepsilon_{xx}^p + d\varepsilon_{yy}^p} = -\frac{\frac{\partial\sigma_y}{\partial\sigma_{xx}}\sin^2\theta + \frac{\partial\sigma_y}{\partial\sigma_{yy}}\cos^2\theta - \frac{\partial\sigma_y}{\partial\tau_{xy}}\sin\theta\cos\theta}{\frac{\partial\sigma_y}{\partial\sigma_{xx}} + \frac{\partial\sigma_y}{\partial\sigma_{yy}}} \tag{23}$$

$$R_b = \frac{d\varepsilon_{yy}^p}{d\varepsilon_{xx}^p} = \frac{\frac{\partial\sigma_y}{\partial\sigma_{yy}}}{\frac{\partial\sigma_y}{\partial\sigma_{xx}}} \tag{24}$$

To calibrate the yield function of MB-1, the following error function in Eq. (25) is defined. By minimizing with Downhill Simplex Method, unknown coefficients of MB-1 are determined.

$$\begin{aligned} Error = &\sum_{i=0}^{90^\circ}\left[\frac{\left(\sigma_i^T\right)^{pred.}}{\left(\sigma_i^T\right)^{exp.}} - 1\right]^2 + \left[\frac{\left(\sigma_b^T\right)^{pred.}}{\left(\sigma_b^T\right)^{exp.}} - 1\right]^2 + \sum_{i=0}^{90^\circ}\left[\frac{\left(\sigma_i^C\right)^{pred.}}{\left(\sigma_i^C\right)^{exp.}} - 1\right]^2 \\ &+ \left[\frac{\left(\sigma_b^C\right)^{pred.}}{\left(\sigma_b^C\right)^{exp.}} - 1\right]^2 + \sum_{i=0}^{90^\circ}\left[\frac{\left(R_i^T\right)^{pred.}}{\left(R_i^T\right)^{exp.}} - 1\right]^2 + \left[\frac{\left(R_b^T\right)^{pred.}}{\left(R_b^T\right)^{exp.}} - 1\right]^2 \\ &+ \sum_{i=0}^{90^\circ}\left[\frac{\left(R_i^C\right)^{pred.}}{\left(R_i^C\right)^{exp.}} - 1\right]^2 + \left[\frac{\left(R_b^C\right)^{pred.}}{\left(R_b^C\right)^{exp.}} - 1\right]^2 \end{aligned} \tag{25}$$

3.2 Calibration of MB-2

Increments of plastic strains, in this case, are computed with aid of plastic potential function. Uniaxial and equi-biaxial Lankford ratios are defined as Eqs. (23) and (24) based on the biaxial tensile or compressive yield stress. Therefore, R_θ^T,R_b^T, R_θ^C and R_b^C are achieved by replacing σ_p instead of σ_y in Eqs. (23) and (24) with the same procedure which was explained in the previous section. To calibrate the yield and plastic potential functions, the following error functions in Eq. (26), *Errorσ* and in Eq. (27), *ErrorR* are defined. By minimizing with the Downhill Simplex Method, the unknown coefficients of yield and plastic potentials functions of MB-2 are determined.

$$Error\sigma = \sum_{i=0}^{90^\circ}\left[\frac{(\sigma_i^T)^{pred.}}{(\sigma_i^T)^{\exp.}} - 1\right]^2 + \sum_{i=0}^{90^\circ}\left[\frac{(\sigma_i^C)^{pred.}}{(\sigma_i^C)^{\exp.}} - 1\right]^2 + \left[\frac{(\sigma_b^T)^{pred.}}{(\sigma_b^T)^{\exp.}} - 1\right]^2 + \left[\frac{(\sigma_b^C)^{pred.}}{(\sigma_b^C)^{\exp.}} - 1\right]^2 = 0 \tag{26}$$

and,

$$ErrorR = \sum_{i=0}^{90^\circ}\left[\frac{(R_i^T)^{pred.}}{(R_i^T)^{\exp.}} - 1\right]^2 + \sum_{i=0}^{90^\circ}\left[\frac{(R_i^C)^{pred.}}{(R_i^C)^{\exp.}} - 1\right]^2 + \left[\frac{(R_b^T)^{pred.}}{(R_b^T)^{\exp.}} - 1\right]^2 + \left[\frac{(R_b^C)^{pred.}}{(R_b^C)^{\exp.}} - 1\right]^2 = 0 \tag{27}$$

3.3 Comparing the errors of MB-1 and MB-2 with experimental results

The accuracies of MB-1 and MB-2 are investigated by the following statements in Eqs. (28) and (29). Here, E_σ^T, E_σ^C, E_b^T and E_b^C compute the errors of predicted uniaxial tensile, compressive yield stresses along with and equi-biaxial tensile and compressive yield stresses with respect to experimental results. Moreover, E_R^T, E_R^C, E_{Rb}^T and E_{Rb}^C calculate the errors of predicted Lankford ratios under tensile and compressive yield stresses along with the Lankford ratios under equi-biaxial tensile and compressive yield stresses with respect to the experimental results. In Eqs. (28) and (29), n is the number of the experimental tests.

$$\begin{cases} E_\sigma^T = \dfrac{1}{n}\sqrt{\displaystyle\sum_{i=0}^{90^\circ}\left(\frac{(\sigma_i^T)_{\exp.} - (\sigma_i^T)_{pred.}}{(\sigma_i^T)_{\exp.}}\right)^2} \times 100 \\ E_\sigma^C = \dfrac{1}{n}\sqrt{\displaystyle\sum_{i=0}^{90^\circ}\left(\frac{(\sigma_i^C)_{\exp.} - (\sigma_i^C)_{pred.}}{(\sigma_i^C)_{\exp.}}\right)^2} \times 100 \\ E_b^T = \dfrac{\left|(\sigma_b^T)_{\exp.} - (\sigma_b^T)_{pred.}\right|}{(\sigma_b^T)_{\exp.}} \times 100 \\ E_b^C = \dfrac{\left|(\sigma_b^C)_{\exp.} - (\sigma_b^C)_{pred.}\right|}{(\sigma_b^C)_{\exp.}} \times 100 \end{cases} \tag{28}$$

and,

$$\begin{cases} E_R^T = \dfrac{1}{n}\sqrt{\displaystyle\sum_{i=0}^{90^\circ}\left(\frac{(R_i^T)_{\exp.} - (R_i^T)_{pred.}}{(R_i^T)_{\exp.}}\right)^2} \times 100 \\ E_R^C = \dfrac{1}{n}\sqrt{\displaystyle\sum_{i=0}^{90^\circ}\left(\frac{(R_i^C)_{\exp.} - (R_i^C)_{pred.}}{(R_i^C)_{\exp.}}\right)^2} \times 100 \\ E_{Rb}^T = \dfrac{\left|(R_b^T)_{\exp.} - (R_b^T)_{pred.}\right|}{(R_b^T)_{\exp.}} \times 100 \\ E_{Rb}^C = \dfrac{\left|(R_b^C)_{\exp.} - (R_b^C)_{pred.}\right|}{(R_b^C)_{\exp.}} \times 100 \end{cases} \tag{29}$$

4 Results and discussions

Different alloys consist of AA 2008-T4, AA 2090-T3, AZ31 B, ZK61 M, high-purity α-titanium, texture magnesium, Mg-0.5% Th alloy, Mg-4% Li alloy and Ti–4 Al–1/4 O2 titanium alloy are selected as case studies here to check the accuracy of MB-1 and MB-2.

4.1 Application to AA 2008-T4 and AA 2090-T3

AA 2008-T4 and AA 2090-T3 are two anisotropic aluminum alloys which have FCC anisotropic structure. The mechanical properties of these materials are reported here. In Table 1a tensile yield stresses and tensile equi-biaxial stress are stated and in Table 1b compressive yield stresses and compressive equi-biaxial stresses are shown, and finally Table 1c shows the Lankford ratios under tensile yield stresses and under equi-biaxial tensile yield stresses. Due to having 24 experiential data points for AA 2008-T4 and AA 2090-T3 as in Table 1, it is considered $n=4$ for MB-1 in Eq. (7). The 24 unknown coefficients of MB-1 are $c'_{1i}, c'_{2i}, c'_{3i}, c'_{6i}, d_{xxi}$ and d_{yyi} for $(i = 1, 2, 3, 4)$ obtained by calibration of MB-1 with 24 experimental results. Now, an error function based on Eq. (25) can be constructed in which $\sigma_i^T, \sigma_i^C, \sigma_b^T, \sigma_b^C, R_i^T$ and R_b^T are computed from Eqs. (12, 15, 19, 22, 23 and 24), respectively and experimental results in Table 1. It is mentioned that the derivatives of stress component for the MB-1 are computed from Eq. (8). Hence, by minimizing the presented error function in Eq. (5) the unknown coefficients of MB-1 can be obtained.

For MB-2, the experimental yield stresses are needed to calibrate the yield function and also the experimental Lankford ratios are required for the plastic potential function. Here, with 16 experimental yield stresses, it is

Table 1 Experimental yield stresses and Lankford ratios of AA 2008-T4 and AA 2090-T3 [19]

a

Material	σ_0^T	σ_{15}^T	σ_{30}^T	σ_{45}^T	σ_{60}^T	σ_{75}^T	σ_{90}^T	σ_b^T
Al 2008-T4	211.67	211.33	208.5	200.03	197.3	194.3	191.56	185.0
Al 2090-T3	279.62	269.72	255	226.77	227.5	247.2	254.45	289.4

b

Material	σ_0^C	σ_{15}^C	σ_{30}^C	σ_{45}^C	σ_{60}^C	σ_{75}^C	σ_{90}^C	σ_b^C
Al 2008-T4	213.79	219.15	227.55	230.25	222.75	220.65	214.64	214.64
Al 2090-T3	248.02	260.75	255	237.75	245.75	263.75	266.48	247.5

c

Material	R_0^T	R_{15}^T	R_{30}^T	R_{45}^T	R_{60}^T	R_{75}^T	R_{90}^T	R_b^T
Al 2008-T4	0.87	0.814	0.634	0.5	0.508	0.506	0.53	1.000
Al 2090-T3	0.21	0.33	0.69	1.58	1.05	0.55	0.69	0.670

considered $n=3$ for the yield function and with 8 experimental Lankford ratios, it is considered here $n=2$ for the plastic potential function. In the yield function, it is assumed that $d_{xx3} = d_{yy3} = 0$ and in the plastic potential function, it is assumed that $c''_{32} = c''_{62} = \overline{d}_{xx2} = \overline{d}_{yy2} = 0$. Finally, it can be stated that, 16 unknown coefficients of yield function are c'_{1i}, c'_{2i}, c'_{3i}, c'_{6i}, d_{xxi} and d_{yyi} for $(i = 1, 2)$ and c'_{13}, c'_{23}, c'_{33} and c'_{63} and 8 unknown coefficients of plastic potential function are c''_{11}, c''_{21}, c''_{31}, c''_{61}, $\overline{d}_{xx1}$, $\overline{d}_{yy1}$, c''_{12} and c''_{22}.

Two error functions are constructed as Eqs. (26) and. (27). In the first one, the yield function of MB-2 is calibrated and σ_i^T, σ_i^C, σ_b^T, σ_b^C are computed and in the second one, the plastic potential function of MB-2 is calibrated and finally, R_i^T and R_b^T can be computed. By minimizing the error functions of Eqs. (26) and (27) the unknown coefficients for yield and plastic potential functions can be are found.

After determining the unknown coefficients of yield functions of AA 2008-T4 and AA 2090-T3 with MB-1 and MB-2, the obtained outcomes are compared with the experimental results, Fig. 1. As it observed MB-1 and MB-2 can predict the experimental data of AA 2008-T4 nearly successfully while MB-2 is more accurate than MB-1 in the prediction of the yield function of AA 2090-T3 in $\sigma_{xx} - \sigma_{yy}$ plane. The plastic potential functions of AA 2008-T4 and AA 2090-T3 of MB-2 can be shown in $\sigma_{xx} - \sigma_{yy}$ plane and it is observed that both plastic potential surfaces are convex similar to the yield functions in Figs. 1, 2.

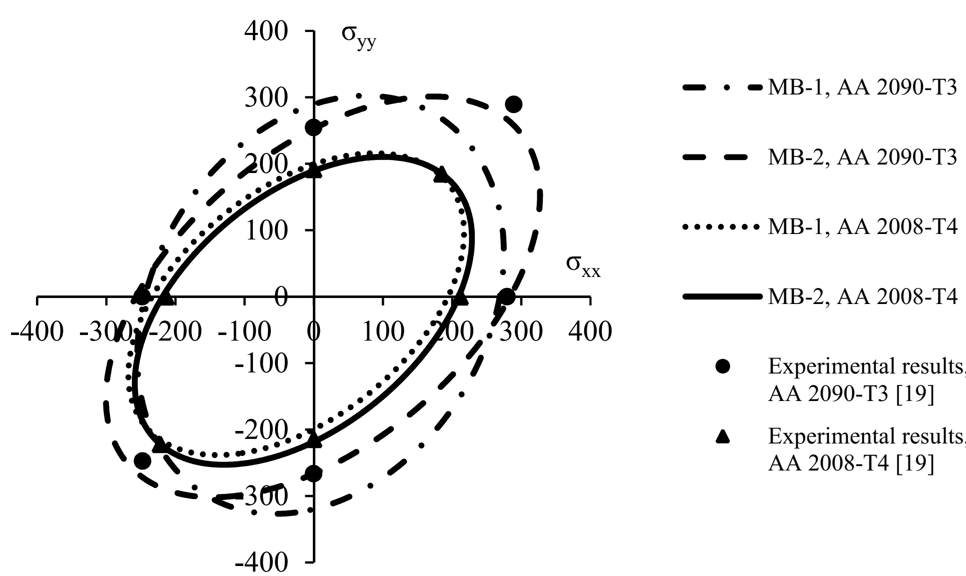

Fig. 1 Comparing the yield function of AA 2008-T4 and AA 2090-T3 with MB-1, MB-2 and experimental results

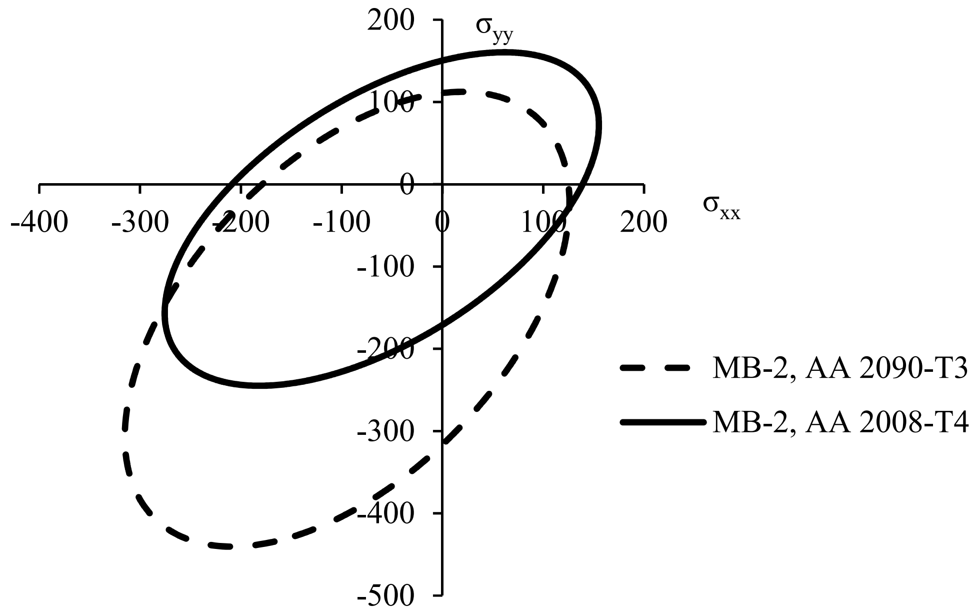

Fig. 2 Plastic potential of AA 2008-T4 and AA 2090-T3 with MB-2

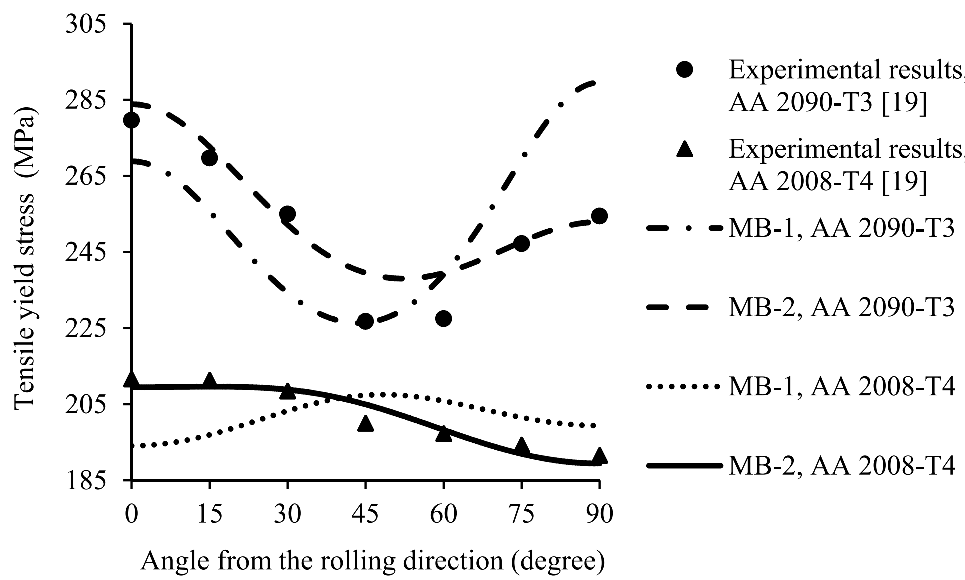

Fig. 3 Comparing the tensile yield stresses of AA 2008-T4 and AA 2090-T3 with MB-1, MB-2 and experimental results

Figures 3 and 4 show the tensile and compressive uniaxial directional yield stresses in Eq. (12) and Eq. (15) of AA 2008-T4 and AA 2090-T3 with MB-1, MB-2. It is seen that in both materials, MB-2 predicts the experimental results more accurate than MB-1. Figure 5 displays the Lankford ratios under tensile uniaxial directional yield stresses of AA 2008-T4 and AA 2090-T3 with MB-1 and MB-2. The difference between MB-1 and MB-2 is very minor in this case.

To compare the MB-1 and MB-2 with experimental data more accurately, root mean square errors (RMSE) are computed as Eqs. (28) and (29) in Table 2. It is observed that RMSE of MB-2 is less than MB-1 compared to the experimental results for both materials. It can be seen that the RMSE of MB criterion in AA 2008-T4 is less than that of AA 2090-T3 due to more difference in value of tensile and compressive mechanical properties and also MB-2 is more accurate than MB-1 in both materials, Table 2.

The initial yield surface is not sufficient for the correctness of a selected function and it is important to find the subsequent yield surface. Therefore, the following case studies are selected in the following.

4.2 Application to AZ31-B and ZK61-M

The experimental tensile and compressive yield stresses, the Lankford ratios under uniaxial tension a compression, the equi-biaxial tensile yield stress and Lankford ratio under

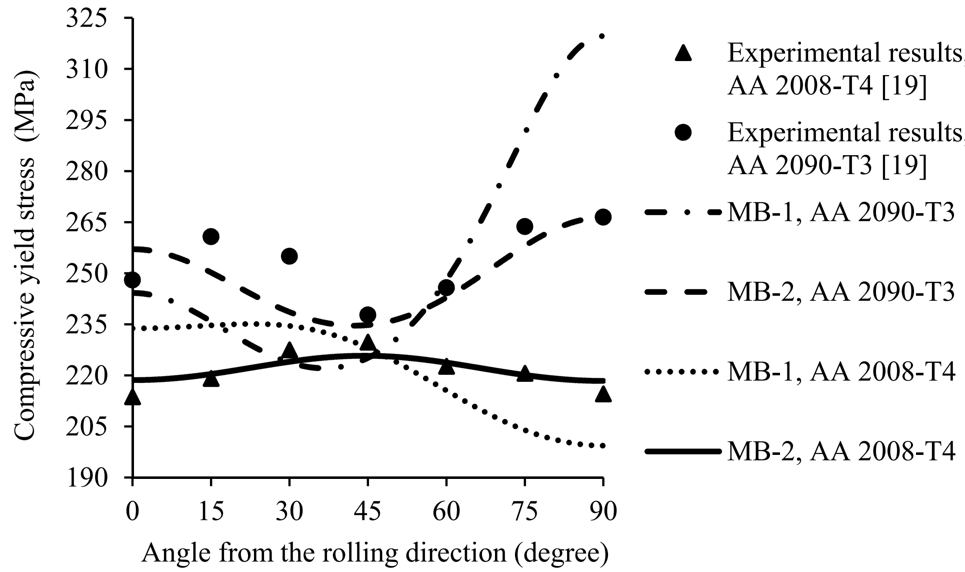

Fig. 4 Comparing the compressive yield stresses of AA 2008-T4 and AA 2090-T3 with MB-1, MB-2 and experimental results

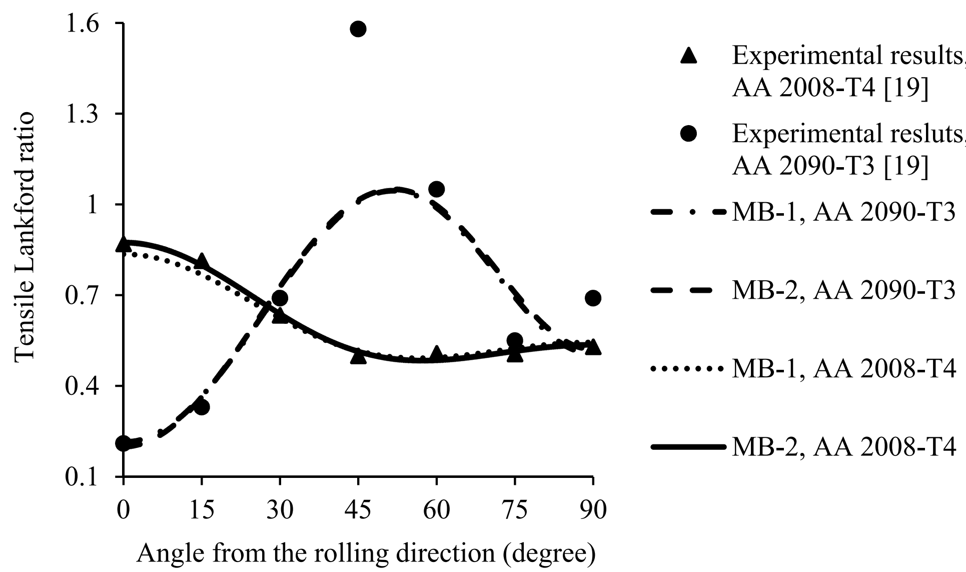

Fig. 5 Comparing the Lankford ratios of AA 2008-T4 and AA 2090-T3 with MB-1, MB-2 and experimental results

Table 2 Comparison of RMSE of MB-1 and MB-2 with experimental data points in percentage

Criterion	$E_{\sigma}^{T}(\%)$	$E_{\sigma}^{C}(\%)$	$E_{R}^{T}(\%)$	$E_{b}^{T}(\%)$	$E_{b}^{C}(\%)$	$E_{Rb}^{T}(\%)$
Al 2008-T4 (MB-1)	1.9392	2.3317	1.3366	1.0601	1.8356	5.4438
Al 2008-T4 (MB-2)	0.4678	0.5399	0.8676	0.0211	0.0036	0.6051
Al 2090-T3 (MB-1)	2.8762	3.9859	7.6545	21.6868	9.4550	10.9442
Al 2090-T3 (MB-2)	1.1487	1.2639	7.6849	5.8599	5.2960	0.9595

equi-biaxial tensile yield stress for different effective plastic strain ratios are shown in Table 6. Using MB-1 causes large value of RMSE.

Therefore, MB-2 is selected for investigation of subsequent yield surfaces of AZ31-B and ZK61-M. It is considered here $n=2$ for the yield function in Eq. (7) with $d_{yy2} = 0$ and also $n=2$ for the plastic potential function with $\overline{d}_{yy2} = 0$.

Using error functions of Eq. (26) and Eq. (27) and mechanical properties in Table 3 and also Eqs. (12, 15, 19, 22, 23 and 24), unknown coefficients of the yield and plastic potential functions of MB-2 are achieved for AZ31-B. Figure 6 shows the subsequent yield surfaces for different effective plastic strains percentage. It is observed that the experimental data

Table 3 Experimental tensile and compressive yield stresses and Lankford ratios of AZ31-B and ZK61-M [32]

a

Material	σ_0^T	$\sigma_{22.5}^T$	σ_{45}^T	$\sigma_{67.5}^T$	σ_{90}^T	σ_0^C	$\sigma_{22.5}^C$	σ_{45}^C	$\sigma_{67.5}^C$	σ_{90}^C
AZ31-B $\bar{\varepsilon}^p = 2\%$	262.966	258.507	242.908	248.407	249.865	159.117	166.128	174.542	152.544	156.082
AZ31-B $\bar{\varepsilon}^p = 4\%$	283.601	279.358	264.547	269.049	271.547	196.516	202.290	211.682	191.444	195.600
AZ31-B $\bar{\varepsilon}^p = 8\%$	309.797	305.839	292.844	298.216	302.847	322.672	334.111	340.882	311.605	318.108
ZK61-M $\bar{\varepsilon}^p = 2\%$	278.458	253.771	184.724	181.804	165.377	172.924	182.154	165.754	216.976	273.159
ZK61-M $\bar{\varepsilon}^p = 4\%$	297.537	277.5103	203.0742	209.5004	200.934	201.915	227.299	205.501	270.383	302.0

b

Material	R_0^T	$R_{22.5}^T$	R_{45}^T	$R_{67.5}^T$	R_{90}^T	R_0^C	$R_{22.5}^C$	R_{45}^C	$R_{67.5}^C$	R_{90}^C
AZ31-B $\bar{\varepsilon}^p = 2\%$	0.928	1.126	1.505	1.323	1.186	0.231	0.105	0.162	0.298	0.110
AZ31-B $\bar{\varepsilon}^p = 4\%$	1.166	1.384	1.817	1.662	1.509	0.336	0.180	0.261	0.390	0.163
AZ31-B $\bar{\varepsilon}^p = 8\%$	1.348	1.580	2.164	1.954	1.832	0.637	0.418	0.515	0.700	0.380
ZK61-M $\bar{\varepsilon}^p = 2\%$	0.952	1.044	1.264	0.580	0.237	0.155	1.600	1.400	1.900	0.479
ZK61-M $\bar{\varepsilon}^p = 4\%$	1.205	1.230	1.589	0.587	0.230	0.200	1.600	1.350	1.800	0.430

c

Material	σ_b^T	R_b^T
AZ31-B $\bar{\varepsilon}^p = 2\%$	226.560	0.81
AZ31-B $\bar{\varepsilon}^p = 4\%$	310.268	0.81
AZ31-B $\bar{\varepsilon}^p = 8\%$	391.963	0.81
ZK61-M $\bar{\varepsilon}^p = 2\%$	242.386	1.795
ZK61-M $\bar{\varepsilon}^p = 4\%$	312.072	1.795

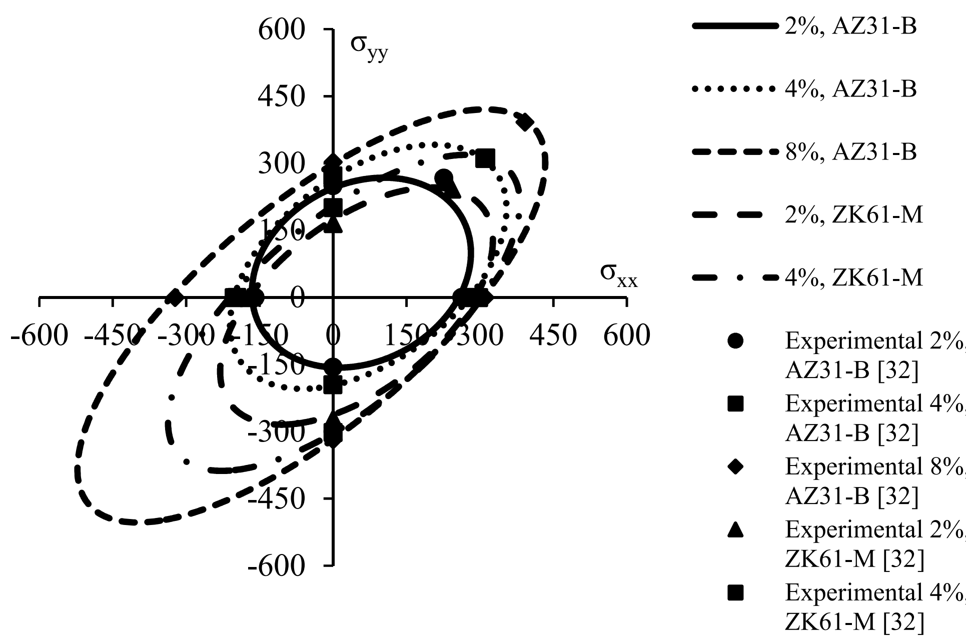

Fig. 6 Comparing the yield function of AZ31-B and ZK61-M with MB-2 and experimental results

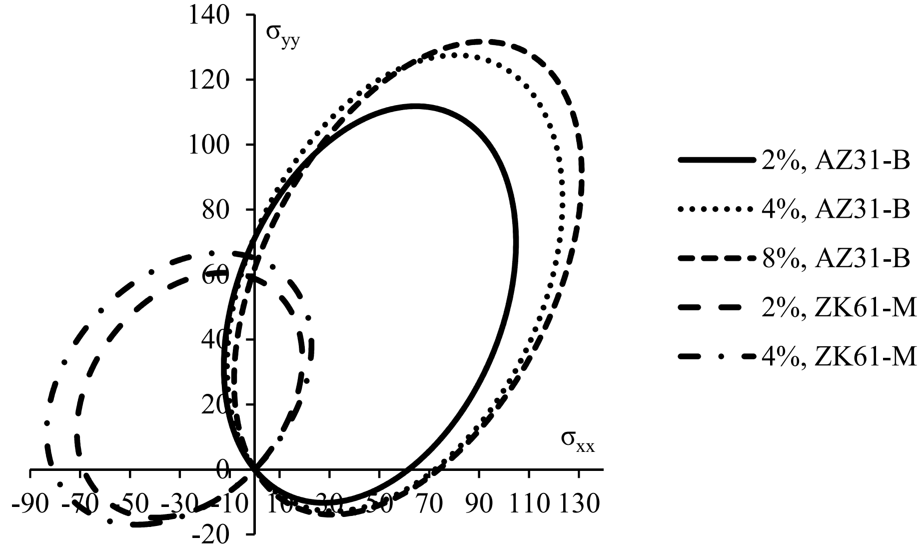

Fig. 7 Plastic potential of AZ31 B and ZK61 M with MB-2

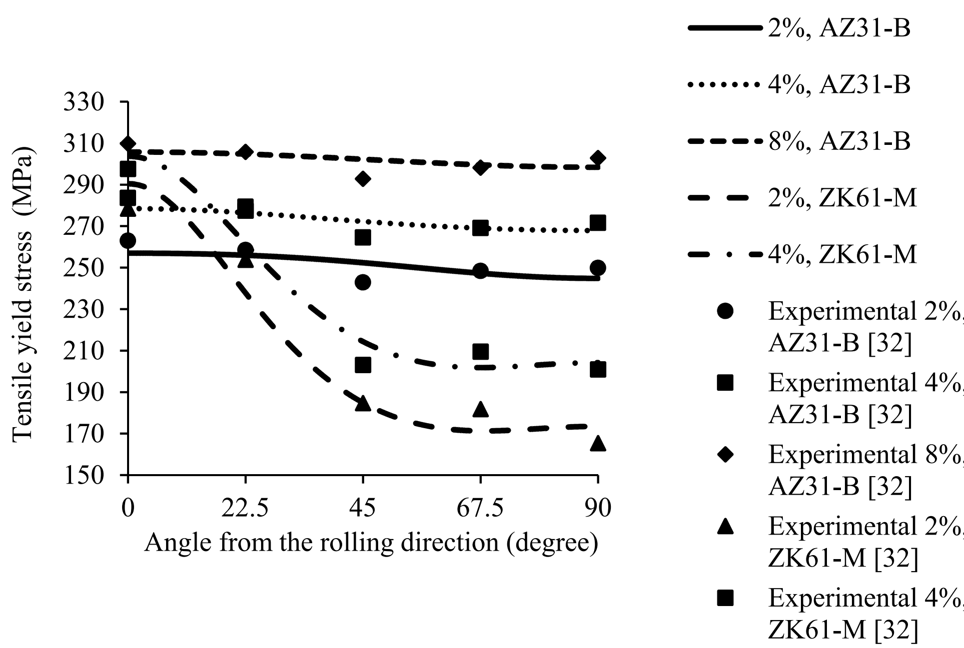

Fig. 8 Comparing the tensile yield stresses of AZ31-B and ZK61-M with MB-2 and experimental results

are well predicted even in subsequent yield surfaces in $\sigma_{xx} - \sigma_{yy}$ plane for both materials.

It is seen that by increasing the value of $\overline{\varepsilon}^p$ the size of plastic surfaces increases and all plastic potentials surfaces are convex, Figs. 6, 7. The directional tensile and compressive yield stresses in comparison of experimental results for AZ31-B and ZK61-M may also be observed which shows the experimental results are anticipated with the proper accuracy, Figs. 8, 9. The Lankford ratios under directional tensile and compressive yield stresses in comparison to the experimental results are also properly estimated, Figs. 10, 11. More clearly comparison of MB-2 with experimental data may be similarly performed, Eqs. (28, 29) and Table 4. In predicting of uniaxial tensile and compressive directional yield stresses for AZ31-B, the RMSEs are less than 1.5% in all values of $\overline{\varepsilon}^p$. Hence, the MB-2 can successfully predict the directional subsequent yield stresses. Moreover, the RMSEs of equi-biaxial tensile yield stress are less than 1% and for Lankford ratio of equi-biaxial tensile yield stress is less than 8%. Generally, it can be stated that MB-2 predicts uniaxial yield stresses and biaxial yield stress more precisely than uniaxial and bi-axial Lankford ratios. Furthermore, in predicting uniaxial tensile and compressive directional yield stresses, the RMSEs are less than 2.5% for ZK61-M in all value of $\overline{\varepsilon}^p$.

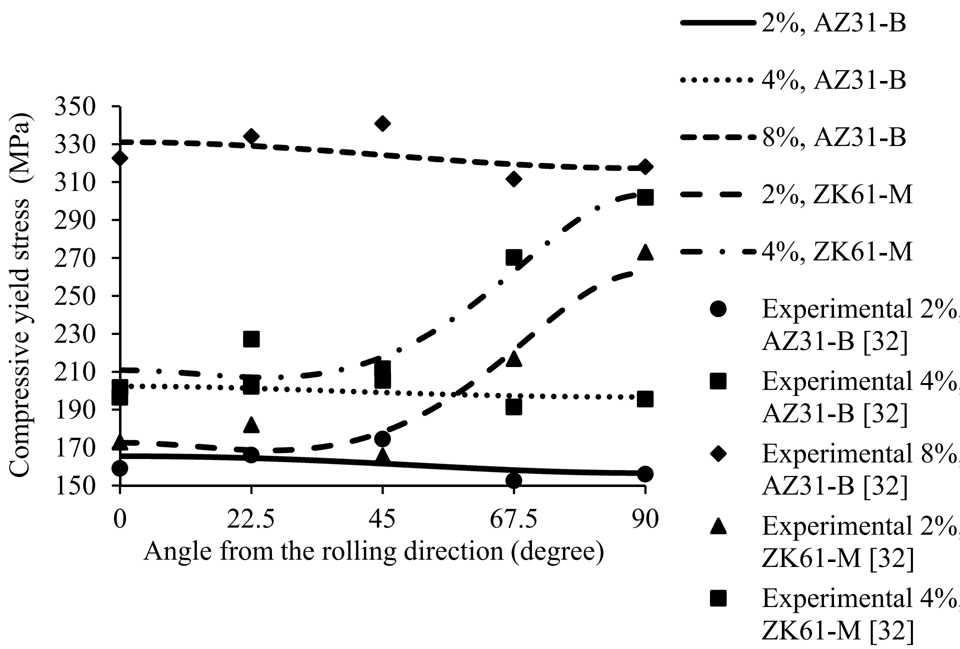

Fig. 9 Comparing the compressive yield stresses of AZ31-B and ZK61-M with MB-2 and experimental results

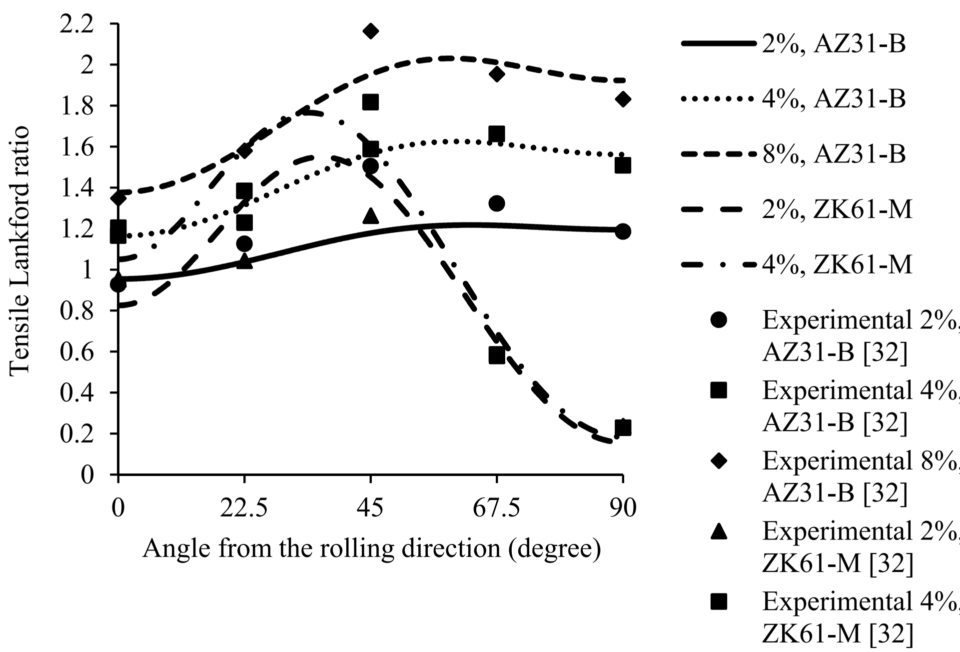

Fig. 10 Comparing the tensile Lankford ratio of AZ31-B and ZK61-M with MB-2 and experimental results

The MB-2 effectively predicted directional subsequent yield stresses. In predicting of Lankford ratios under directional tensile and compressive uniaxial yield stresses RMSEs become larger than yield stresses. RMSEs of equi-biaxial tensile yield stress are less than 0.5% but RMSEs of Lankford ratios under equi-biaxial tensile yield stress RMSEs become very large. It can be reported that, the MB-2 is a proper criterion for ZK61-M in predicting uniaxial yield stresses and biaxial yield stress rather than uniaxial and biaxial Lankford ratios.

4.3 Application to High-Purity *α*-Titanium

Tensile and compressive yield stresses of high-purity α-titanium along with the tensile and compressive equi-biaxial yield stresses are given in Table 5. In this section, with havening no data points on directional Lankford ratios, MB-1 and MB-2 have a unique result. Therefore, it is called hear MB for investigation of subsequent yield surfaces for high-purity α-titanium.

Due to having mechanical properties in in $\theta = 0°$ and $\theta = 90°$, c'_6 is omitted from the yield function and coefficients

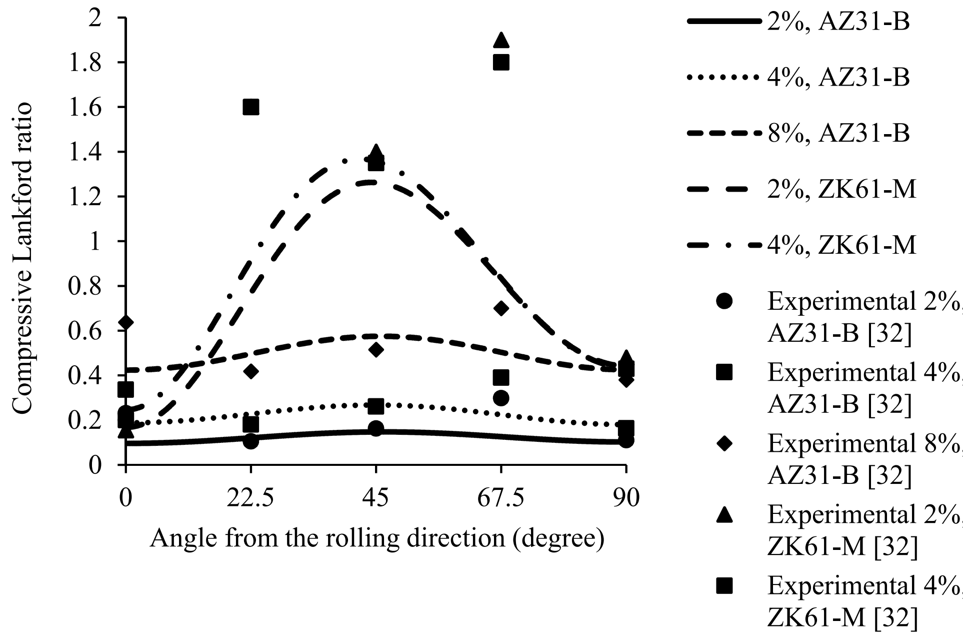

Fig. 11 Comparing the compressive Lankford ratio of AZ31-B with MB-2 and experimental results

Table 4 Comparison of root mean square errors of AZ31-B and ZK61-M with experimental data

Criterion	$E_{\sigma}^{T}(\%)$	$E_{\sigma}^{C}(\%)$	$E_{R}^{T}(\%)$	$E_{R}^{C}(\%)$	$E_{b}^{T}(\%)$	$E_{Rb}^{T}(\%)$
AZ31-B $\bar{\varepsilon}^{p} = 2\%$	1.0101	1.8528	4.9244	16.8179	0.4002	4.1061
AZ31-B $\bar{\varepsilon}^{p} = 4\%$	0.7959	1.4700	3.0659	13.5065	0.6370	6.8391
AZ31-B $\bar{\varepsilon}^{p} = 8\%$	0.7603	1.2493	2.3111	10.0873	0.8419	7.8100
ZK61-M $\bar{\varepsilon}^{p} = 2\%$	2.1526	2.2958	9.8211	15.6565	0.3557	35.6277
ZK61-M $\bar{\varepsilon}^{p} = 4\%$	1.8384	2.3817	8.4043	14.4923	0.4024	20.0370

Table 5 The experimental tensile and compressive yield stresses of high-purity α-titanium with $\bar{\varepsilon}^{p} = 0\%, 5\%, 10\%, 20\%$ [19]

$\bar{\varepsilon}^{p}(\%)$	σ_{0}^{T}	σ_{90}^{T}	σ_{b}^{T}	σ_{0}^{C}	σ_{90}^{C}	σ_{b}^{C}
0	152	179	235	148	182	229
5	228	263	328	227	278	301
10	255	281	359	273	310	320
20	294	299	415	385	363	335

c_1', c_2', c_3', d_{xx} and d_{yy} should be computed. Using error functions of Eq. (26) and yield stresses in Table 5 along with Eqs. (12, 15, 19, 22), unknown coefficients of yield function of MB with $n=1$ in Eq. (7) can be obtained. Hence, the yield function is gained and the following discussions can be reported. It is mentioned that the plastic potential function cannot be reached due to having less data on directional Lankford ratios.

Now, subsequent yield surfaces of high-purity α-titanium can be plotted in Fig. 12. As it can be observed, although MB is successful in predicting experimental data but with increasing the plastic zone, the error of predicted experimental results becomes larger. Moreover, for a more comparison of MB with the experimental data, RMSE are computed by Eq. (28), see Table 6. It is seen that with increasing the plastic zone, RMSE becomes larger an all errors are less than 10%. Therefore, MB could successfully predict the subsequent yield stresses.

4.4 Application to textured magnesium, Mg-0.5% Th alloy, Mg-4% Li alloy and Ti–4 Al–1/4 O2 titanium alloy

The experimental tensile and compressive yield stresses along with the tensile equi-biaxial yield stress for textured magnesium, Mg-0.5% Th alloy, Mg-4% Li alloy, and Ti-4 Al-1/4 O2 titanium alloy with $\bar{\varepsilon}^{p} = 1\%, 5\%, 10\%$ are shown in Table 7.

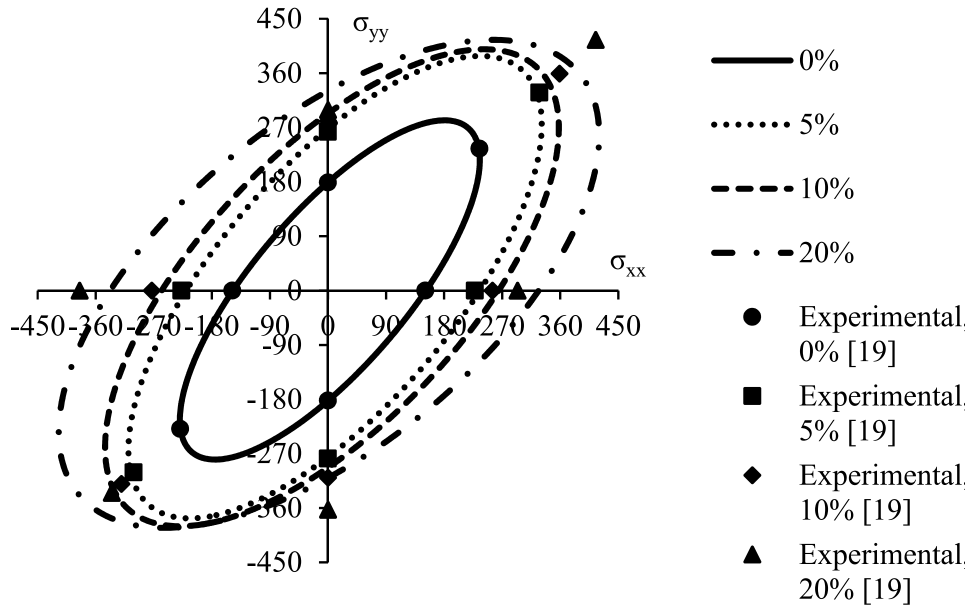

Fig. 12 Comparing the subsequent yield surfaces of high-purity α-titanium with MB and experimental results

Table 6 Comparison the root mean square errors of high-purity α-titanium with experimental data with MB

Criterion	$E_\sigma^T(\%)$	$E_\sigma^C(\%)$	$E_b^T(\%)$	$E_b^C(\%)$
high-purity α-titanium with $\overline{\varepsilon}^p = 0\%$	0.2821	0.2386	0.4190	0.1466
high-purity α-titanium with $\overline{\varepsilon}^p = 5\%$	1.8908	1.6355	1.0183	1.2838
high-purity α-titanium with $\overline{\varepsilon}^p = 10\%$	2.8619	3.8981	4.5226	3.5638
high-purity α-titanium with $\overline{\varepsilon}^p = 20\%$	7.6745	9.5246	9.5761	7.9661

Due to lack of experimental results in the directional Lankford ratios, MB-1 and MB-2 have the same results. Now, MB is studied to investigate subsequent yield surfaces of textured magnesium, Mg-0.5% Th alloy, Mg-4% Li alloy and Ti-4 Al-1/4 O2 titanium alloy with $\overline{\varepsilon}^p = 1\%, 5\%, 10\%$. Because of having mechanical properties in $\theta = 0°$ and $\theta = 90°$, c_6' is omitted from the yield function and coefficients c_1', c_2', c_3', d_{xx} and d_{yy} are computed.

Using error functions of Eq. (26) and yield stresses in Table 7 along with Eqs. (12, 15, 19), the unknown coefficients of yield function of MB with $n = 1$ in Eq. (7) are obtained. It is mentioned that the plastic potential function cannot be found due to not having enough data on the directional Lankford ratios. The yield functions of textured magnesium, Mg-0.5% Th alloy, Mg-4% Li alloy and Ti-4 Al-1/4 O2 titanium alloy with $\overline{\varepsilon}^p = 1\%, 5\%, 10\%$ in $\sigma_{xx} - \sigma_{yy}$ may be found and the experimental results are properly predicted with $\overline{\varepsilon}^p = 1\%, 5\%, 10\%$ in all cases, Fig. 13. The tensile and compressive uniaxial directional and equi-biaxial tensile yield stresses RMSEs are also computed, Table 8. As it is observed, for Texture Magnesium, Mg-0.5% Th alloy and Mg-4% Li alloy, the RMSEs are less than 0.5% and for Ti-4 Al-1/4 O2 titanium alloy the RMSEs are less than 4%. Therefore, the MB is a proper criterion to forecast yield function of these materials with $\overline{\varepsilon}^p = 1\%, 5\%, 10\%$ in $\sigma_{xx} - \sigma_{yy}$ plane.

5 Conclusions

In this study, the Burzynski criterion is modified for asymmetric anisotropic materials called hear MB. Yielding of different alloys such as AA 2008-T4 and AA 2090-T3 with

Table 7 The experimental tensile and compressive yield stresses of, **a** textured magnesium [unit: ksi], **b** Mg-0.5% Th alloy [unit: MPa], **c** Mg-4% Li alloy [unit: MPa], **d** Ti-4 Al-1/4 O2 titanium alloy [unit: MPa] with $\overline{\varepsilon}^p = 1\%,\ 5\%,\ 10\%$ [18]

a

$\overline{\varepsilon}^p(\%)$	σ_0^T	σ_b^T	σ_{90}^T	σ_0^C	σ_{90}^C
1	10.08	9.47	18.93	4.00	3.95
5	18.95	18.01	23.86	8.00	10.04
10	22.95	21.80	28.80	21.39	25.34

b

$\overline{\varepsilon}^p(\%)$	σ_0^T	σ_b^T	σ_{90}^T	σ_0^C	σ_{90}^C
1	188.28	150.61	167.194	96.65	100.79
5	208.36	196.95	200.39	125.52	129.24
10	215.90	214.63	221.73	212.13	199.20

c

$\overline{\varepsilon}^p(\%)$	σ_0^T	σ_b^T	σ_{90}^T	σ_0^C	σ_{90}^C
1	93.75	93.99	79.36	66.66	67.46
5	138.54	157.51	121.03	94.79	95.23
10	153.12	191.54	151.78	151.04	148.81

d

$\overline{\varepsilon}^p(\%)$	σ_0^T	σ_b^T	σ_{90}^T	σ_0^C	σ_{90}^C
1	656.25	955.78	677.41	596.59	532.25
5	698.86	1121.91	709.67	758.52	725.80
10	775.56	1300.61	750.00	869.31	879.03

Face-Centered Cubic (FCC structure) and also AZ31 B, ZK61 M, high purity α-titanium, texture magnesium, Mg-0.5% Th alloy, Mg-4% Li alloy and Ti-4 Al-1/4 O2 titanium alloy with Hexagonal Close-Packed (HCP structure) are studied and RMSEs are computed to show the accuracy of MB-1 and MB-2. Finally, it is shown that MB-2, effectively depicts the behavior of pressure-sensitive anisotropic materials compared to experimental results in a new approach. Some important outcomes are as follows:

1. The modified deviatoric stress tensor is defined with a linear transformation to consider the anisotropy effects of materials.
2. Yield function of MB-1 and also yield and plastic potential functions of MB-2 are presented by sum of n-components to have more capability to be calibrated with different numbers of experimental tests.
3. The non-linear effect of hydrostatic pressure is neglected due to the previous experiments stated that the yielding of anisotropic materials linearly depends on hydrostatic pressure.

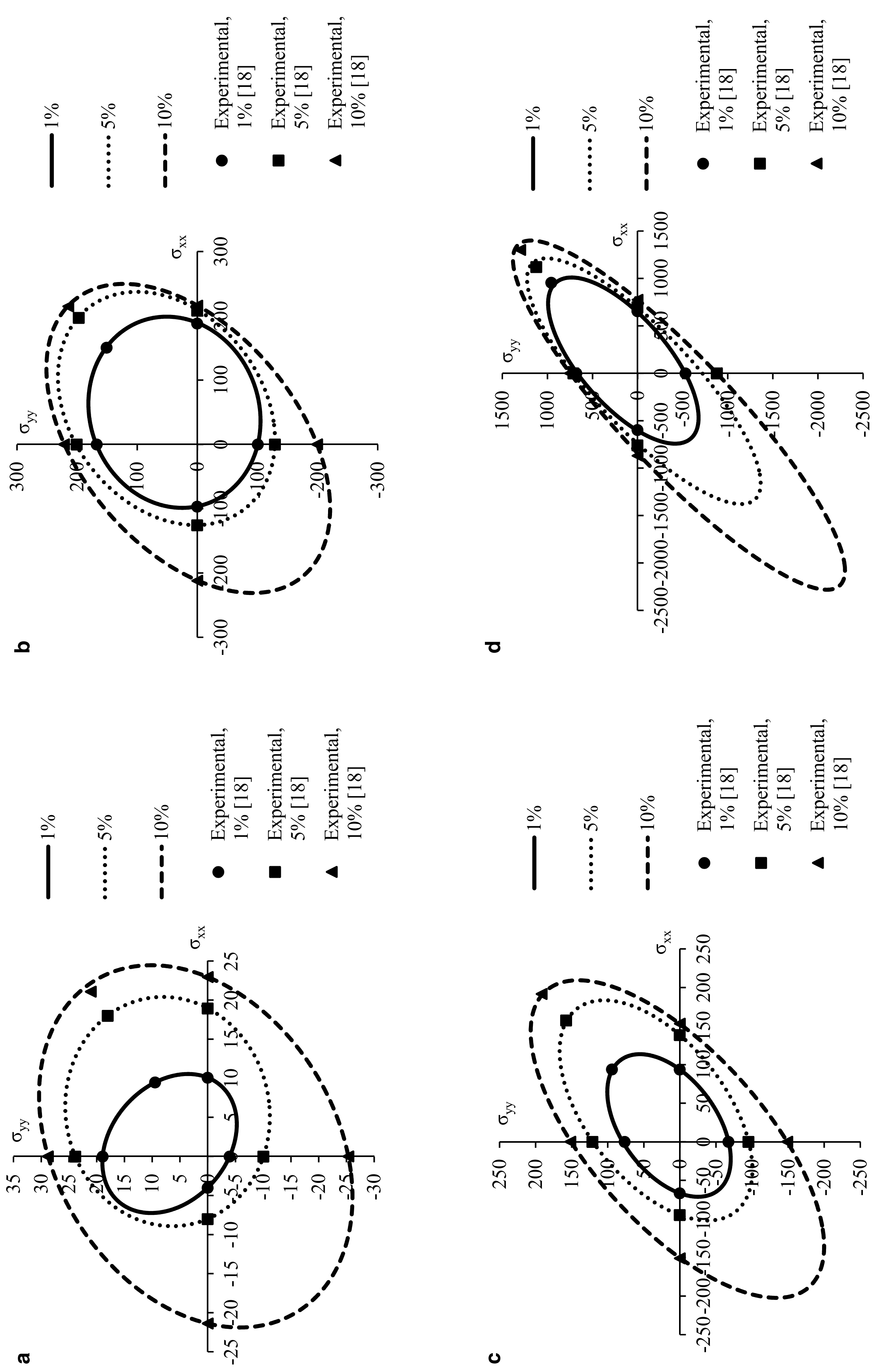

Fig. 13 Comparing the subsequent yield surfaces of, **a** texture magnesium, **b** Mg-0.5% Th alloy, **c** Mg-4% Li alloy, **d** Ti-4 Al-1/4 O2 titanium alloy with MB and experimental results

Table 8 Comparison of root mean square errors of textured magnesium, Mg-0.5% Th alloy, Mg-4% Li alloy and Ti-4 Al-1/4 O2 titanium alloy with experimental data

Criterion	$E_{\sigma}^{T}(\%)$	$E_{\sigma}^{C}(\%)$	$E_{b}^{T}(\%)$
Texture Magnesium $\bar{\varepsilon}^{p} = 1\%$	0.0090	0.0066	0.0042
Texture Magnesium $\bar{\varepsilon}^{p} = 5\%$	0.0097	0.0248	0.0040
Texture Magnesium $\bar{\varepsilon}^{p} = 10\%$	0.0630	0.0108	0.0025
Mg-0.5% Th alloy $\bar{\varepsilon}^{p} = 1\%$	0.2384	0.2419	0.4350
Mg-0.5% Th alloy $\bar{\varepsilon}^{p} = 5\%$	0.4608	0.1145	0.4214
Mg-0.5% Th alloy $\bar{\varepsilon}^{p} = 10\%$	0.1398	0.1470	0.2900
Mg-4% Li alloy $\bar{\varepsilon}^{p} = 1\%$	0.0514	0.1006	0.4329
Mg-4% Li alloy $\bar{\varepsilon}^{p} = 5\%$	0.1805	0.1080	0.3425
Mg-4% Li alloy $\bar{\varepsilon}^{p} = 10\%$	0.3091	0.1952	0.3971
Ti-4 Al-1/4 O2 titanium alloy $\bar{\varepsilon}^{p} = 1\%$	1.1258	0.8081	2.5660
Ti-4 Al-1/4 O2 titanium alloy $\bar{\varepsilon}^{p} = 5\%$	0.7308	1.1076	3.6636
Ti-4 Al-1/4 O2 titanium alloy $\bar{\varepsilon}^{p} = 10\%$	0.2452	1.4729	2.9942

Declarations

Conflict of interest We wish to draw the attention of the Editor to the following facts which may be considered as potential conflicts of interest to this work. We confirm that the manuscript entitled "Modified Burzynski criterion along with AFR and non-AFR for asymmetric anisotropic materials" has been read and approved by all named authors and that there are no other persons who satisfied the criteria for authorship but are not listed. We further confirm that the order of authors listed in the manuscript has been approved by all of us. We confirm that we have given due consideration to the protection of intellectual property associated with this work and that there are no impediments to publication, including the timing of publication, with respect to intellectual property. In so doing we confirm that we have followed the regulations of our institutions concerning intellectual property. We understand that the Corresponding Author is the sole contact for the Editorial process (including Editorial Manager and direct communications with the office). He is responsible for communicating with the other authors about progress, submissions of revisions, and final approval of proofs. We confirm that we have provided a current, correct email address which is accessible by the Corresponding Author and which has been configured to accept any emails. Signed by all authors.

References

1. Spitzig WA, Sober RJ, Richmond O. Pressure dependence of yielding and associated volume expansion in tempered martensite. ActaMetall. 1975;23:885–93.
2. Spitzig WA, Richmond O. The effect of pressure on the flow stress of metals. ActaMetall. 1984;32:457–63.
3. Barlat F, Brem JC, Yoon JW, Chung K, Dick RE, Lege DJ, Pourboghrat F, Choi SH, Chu E. Plane stress yield function for aluminum alloy sheets-part 1: theory. Int J Plast. 2003;19:1297–319.
4. Stoughton TB, Yoon JW. A pressure-sensitive yield criterion under a non-associated flow rule for sheet metal forming. Int J Plast. 2004;20:705–31.
5. Hu W. An orthotropic criterion in a 3-D general stress state. Int J Plast. 2005;21:1771–96.
6. Pecherski RB. Burzynski yield criterion vis-a-vis the related studies reported in the literature. Eng Trans. 2008;56(4):383–91.
7. Hu W, Wang ZR. Construction of a constitutive model in calculations of pressure-dependent material. Comput Mater Sci. 2009;46:893–901.
8. Stoughton TB, Yoon JW. Anisotropic hardening and non-associated flow in proportional loading of sheet metals. Int J Plast. 2009;25:1777–817.
9. Nixon ME, Cazacu O, Lebensohn RA. Anisotropic response of high-purity -titanium: experimental characterization and constitutive modeling. Int J Plast. 2010;26:516–32.
10. Fras T, Kowalewski Z, Pecherski RB, Rusinek A. Applications of Burzynski failure criteria – I. Isotropic materials with asymmetry of elastic range. Eng Trans. 2010;58(1–2):1–10.
11. Fras T, Pecherski RB. Applications of the Burzynski hypothesis of material effort for isotropic solids. Mech Control. 2010;29(2):45–50.
12. Vadillo G, Fernandez-Saez J, Pecherski RB. Some applications of Burzynski yield condition in metal plasticity. Mater Des. 2011;32:628–35.
13. Nowak M, Ostrowska-Maciejewska J, Pecherski RB, Szeptynski P. Yield criterion accounting for the third invariant of stress tensor deviator. Part I. Proposition of the yield criterion based on the concept of influence functions. Eng Trans. 2011;59(4):273–81.
14. Pecherski RB, Szeptynski P, Nowak M. An extension of Burzynski hypothesis of material effort accounting for the third invariant of stress tensor. Arch Metall Mater. 2011;56(2):503–8.
15. Szeptynski P. Some remarks on Burzynski failure criterion for anisotropic materials. Eng Trans. 2011;59(2):119–36.
16. Ostrowska- Maciejewska J, Pecherski RB, Szeptynski P. Limit condition for anisotropic materials with asymmetric elastic range. Eng Trans. 2012;60(2):125–38.
17. Andar MO, Kuwabara T, Steglich D. Material modeling of AZ31 Mg sheet considering variation of r-values and asymmetry of the yield locus. Mater SciEng A. 2012;549:82–92.
18. Lou Y, Huh H, Yoon JW. Consideration of strength differential effect in sheet metals with symmetric yield functions. Int J Mech Sci. 2013;66:214–23.
19. Yoon JW, Lou Y, Yoon J, Glazoff MV. Asymmetric yield function based on the stress invariants for pressure sensitive metals. Int J Plast. 2014;56:184–202.
20. Moayyedian F, Kadkhodayan M. Combination of modified Yld 2000–2d and Yld2000-2d in anisotropic pressure dependent sheet metals. Latin Am J Solids Struct. 2015;12:92–114.
21. Moayyedian F, Kadkhodayan M. Modified Burzynski criterion with non-associated flow rule for anisotropic asymmetric metals in plane stress problems. Appl Math Mech (English Edition). 2015;36:303–18.
22. Kolupaev VA, Yu MH, Altenbach H. Fitting of the strength hypotheses. Acta Mech. 2016;227:1533–56.
23. Moayyedian F, Kadkhodayan M. An advanced criterion based on non-AFR for anisotropic sheet metals. Struct Eng Mech. 2016;57:1015–38.
24. Moayyedian F, Kadkhodayan M. A modified Burzynski criterion for anisotropic pressure-dependent materials. Sadhana. 2017;42:95–109.
25. Lou Y, Yoon JW. Anisotropic ductile fracture criterion based on linear transformation. Int J Plast. 2017;93:3–25.
26. Moayyedian F, Kadkhodayan M. Non-linear influence of hydrostatic pressure on yielding of asymmetric anisotropic sheet metals. Math Mech Solids. 2018;23:159–80.
27. Suzuki T, Okamura K, Capilla G, Hamasaki H, Yoshida F. Effect of anisotropy evolution on circular and oval hole expansion behavior of high-strength steel sheets. Int J Mech Sci. 2018;146–147:556–70.

28. Lou Y, Yoon JW. Anisotropic yield function based on stress invariants for BCC and FCC metals and its extension to ductile fracture criterion. Int J Plast. 2018;101:125–55.
29. Mucha M, Wcisło B, Pamin J, Kowalczyk-Gajewska K. Instabilities in membrane tension: parametric study for large strain thermoplasticity. Arch Civil MechEng. 2018;18:1055–67.
30. Chandola N, Cazacu O, Revil-Baudard B. Prediction of plastic anisotropy of textured polycrystalline sheets using a new single-crystal model. CR Mec. 2018;346:756–69.
31. Lou Y, Zhang S, Yoon JW. A reduced Yld 2004 function for modeling of anisotropic plastic deformation of metals under triaxial loading. Int J Mech Sci. 2019;161–162:105027.
32. Lia Zh, Yang H, Liu J. Comparative study on yield behavior and non-associated yield criteria of AZ31B and ZK61 M magnesium alloys. Mater SciEng A. 2019;759:329–45.
33. Lou Y, Yoon JW. Alternative approach to model ductile fracture by incorporating anisotropic yield function. Int J Solids Struct. 2019;164:12–24.
34. Wosatko A, Winnicki A, Polak MA, Pamin J. Role of dilatancy angle in plasticity-based models of concrete. Arch Civil MechEng. 2019;19:1–16.
35. Banaszkiewicz M, Dudda W, Badur J. The effect of strength differential on material effort and lifetime of steam turbine rotors under thermo-mechanical load. Eng Trans. 2019;67(2):167–84.
36. Wu B, Wang H, Taylor T, Yanagimoto J. A non-associated constitutive model considering anisotropic hardening for orthotropic anisotropic materials in sheet metal forming. Int J Mech Sci. 2019;169:105320.